AADE-18-FTCE-063

Numerical Modeling of Wellbore Ballooning: Linking Mud Circulation in the Wellbore and Fracture Opening/Closing in the Rock

Yongcun Feng and K. E. Gray, The University of Texas at Austin

Abstract

Wellbore ballooning is commonly observed during drilling. Understanding the mechanisms and factors controlling wellbore ballooning is important for distinguishing it from a kick and avoiding unnecessary operational costs. The drilling industry needs realistic models that can predict and interpret wellbore ballooning. However, challenges exist in modeling this phenomenon because it involves coupling between fracture opening/closing in the formation and dynamic mud circulation pressures in the wellbore. Most wellbore ballooning models are based on analytical methods and assume a pre-existing fracture whose aperture changes with a predefined fluid pressure in the fracture. None of them couple mud circulation in the annulus with fracture mechanics, which is important for capturing realistic wellbore ballooning processes.

In this paper, a novel numerical approach is presented, which for the first time couples dynamic mud circulation and fracture behavior in wellbore ballooning. Mud circulation is modeled based on Bernoulli's equation, taking into account both gravity and viscous pressure losses. Fracture behavior is described using the well-established cohesive zone approach. The model captures drilling mud loses into the formation during mud circulation and flow-back into the wellbore with pumps off. In addition, the model can provide estimates of time-dependent wellbore pressure, fluid loss/gain rate, and the fracture profile.

Introduction

Borehole ballooning is the phenomenon of reversible mud losses and gains during drilling (Lavrov and Tronvoll, 2005). It has been a major, but not well-understood, problem in the drilling industry. Borehole ballooning is an indicator of a likely subsequent lost circulation event. Failure to control borehole ballooning may result in significant fluid loss and, consequently, increased drilling time and cost (Ozdemirtas et al., 2007, 2009). Furthermore, mud gain from a formation in the pump-off period may be diagnosed as a well kick, prompting an increased mud weight to prevent it. This could lead to even worse lost circulation events, especially in high-pressure, high-temperature (HPHT) formations, where the safe drilling margin is narrow and a minor change in mud weight can cause wellbore failure (Feng et al., 2015; Feng and Gray, 2016, 2017; Helstrup et al., 2004). On the other hand, borehole ballooning also has its valuable aspects. For example, Ziegler and Jones (2014) argued that some information collected from borehole ballooning can be used to constrain the fracture gradient of a wellbore.

Borehole ballooning mostly occurs in naturally fractured formations. During mud circulation, high equivalent circulation density (ECD) in the annulus resulting from additional frictional pressure exceeds reopening pressure of the natural fractures, resulting in mud loss into the formation. With pumps off, the annulus pressure falls below the fracture reopening pressure due to the removal of frictional pressure, and a sizeable amount of mud flows back into the wellbore. An accurate model capturing this process can aid in understating the mechanisms behind borehole ballooning, distinguishing it from a well kick, and improving mud optimization (Bychina et al., 2017; Mehrabi et al., 2012; Shahri et al., 2011).

For a comprehensive borehole ballooning model, three major physical processes should be taken into account and modeled simultaneously. They are wellbore hydraulics, fracture opening/closing, and deformation of porous formation. There is a very limited number of published borehole ballooning models. To the authors' knowledge, none of them couples the three components above.

Sanfillippo et al. (1997) proposed a mud loss model which assumes mud flows into a non-deformable fracture with a constant aperture and impermeable fracture walls. Similarly, Lietard et al. (1999) developed a model for mud flow into a non-deformable, infinite radial fracture. These models, neglecting fracture deformation with pressure buildup inside the fracture, may cause underestimation of fluid loss volume (Bychina et al., 2017). Lavrov and Tronvoll (2004) introduced a borehole ballooning model for fluid loss into a fracture of finite length undergoing fracture aperture change with a linear deformation law. Later, they extended the model to fracture deformation with an exponential deformation law (Lavrov and Tronvoll, 2005). Ozdemirtas et al. (2009) also used a model with a linear fracture deformation law to investigate borehole ballooning with an emphasis on the effect of fracture roughness. Similar models using a linear or exponential deformation law to relate fracture aperture and fluid pressure in the fracture were also presented in Majidi et al. (2010, 2008) and Shahri et al. (2011). None of these models describes the initiation, propagation, and closure of the fractures based on a fracture mechanics theory. Moreover, they do not explicitly model mud circulation in the wellbore as well as rock deformation and pore fluid flow in the bulk formation surrounding the fracture. Therefore they cannot capture fluid exchanges between the wellbore, fracture, and formation during borehole ballooning events.

In this paper, we present a new model, which for the first time couples dynamic mud circulation, fracture opening/closing, and formation deformation during borehole ballooning. The model significantly reduces the shortcomings of previous models. Mud circulation is modeled based on Bernoulli's equation, taking into account both gravity and viscous pressure losses. Fracture behavior is described using the well-established cohesive zone approach. The model captures mud losses into the formation during mud circulation and mud gains from the formation during pump-off period. In addition, the model can provide estimates of time-dependent wellbore pressure, fluid loss/gain rate, and the fracture profile. A numerical example is carried out in this paper to illustrate the capabilities of the new model.

Modeling Theory

Borehole ballooning is modeled using a coupled fluid flow (including fluid flows in the wellbore, fracture, and formation) and geomechanics approach. Finite-element code Abaqus is used to develop the model. As mentioned above, a comprehensive borehole ballooning system should consist of three major components: the wellbore, the hydraulic fracture, and the formation, as illustrated in Fig. 1. The corresponding physical processes in these three components during borehole ballooning include (1) mud circulation in the wellbore, (2) dynamic fracture growth/closure and fracture fluid flow, and (3) deformation and pore fluid flow of the formation. In this section, the theories used to model these three parts are described briefly.

Wellbore Fluid Flow

During drilling, the drilling mud is pump into the wellbore through the drill pipe and circulated out through the annulus, as shown in Fig. 1. The bottom hole pressure in the annulus during mud circulation consists of two parts: the hydrostatic pressure induced by the gravity of the mud column and the viscous pressure losses in the annulus due to fluid flow. Mud circulation in the wellbore is modeled based on Bernoulli's equation (using a Darcy-Weisbach approach) considering both gravity and viscous pressure terms as follows (SIMULIA, 2016; Feng and Gray, 2017b)

$$\Delta P - \rho g \Delta Z = C_L \frac{\rho v^2}{2} \tag{1}$$

$$C_L = \frac{fL}{D_h} \tag{2}$$

$$D_h = \frac{4A}{S} \tag{3}$$

where, ΔP is the pressure difference between the two points; ΔZ is the elevation difference between two points; v is the fluid velocity in the pipe; ρ is the fluid density; g is the gravity acceleration factor; C_L is the loss coefficient; L is the pipe length; f is the friction factor; D_h is the hydraulic diameter of the pipe; A is the cross-sectional area of the pipe; and S is the wetted perimeter of the pipe.

The friction factor f in Eq. 2 is an important parameter which determines the friction loss during fluid flow. In the simulation, the friction factor is determined by the Churchill friction loss formula (Churchill, 1977)

$$f = 8\left[\left(\frac{8}{Re}\right)^{12} + \frac{1}{(A+B)^{1.5}}\right]^{\frac{1}{12}} \tag{4}$$

where $A = \left[-2.457 ln\left(\left(\frac{7}{Re}\right)^{0.9} + 0.27\frac{K_s}{D_h}\right)\right]^{16}$; $B = \left(\frac{37350}{Re}\right)^{16}$; Re is Reynolds number; K_s is roughness of the pipe.

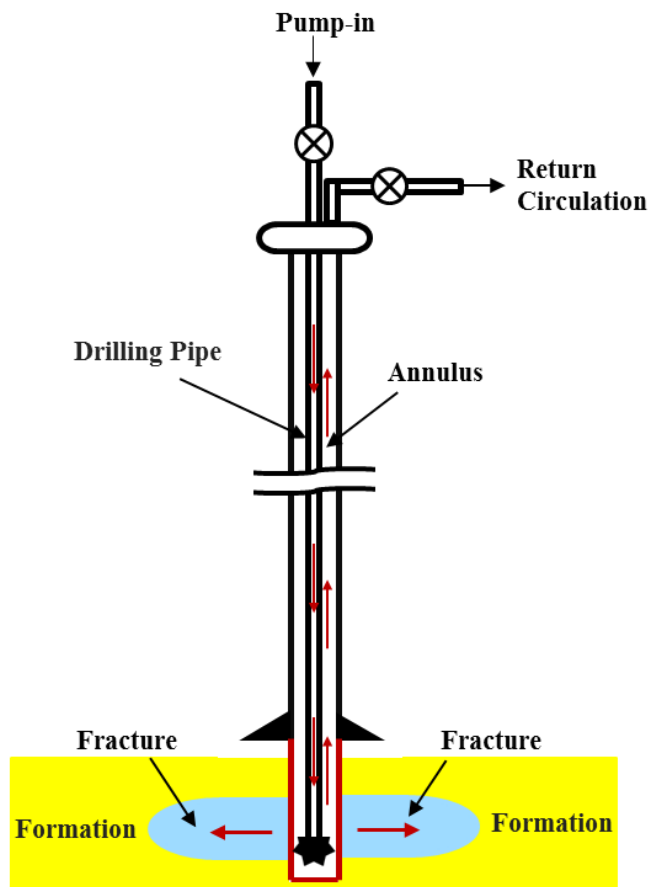

Fig. 1 Diagram of the borehole ballooning system. Three major components of the system include the wellbore, the fracture, and the formation.

Fracture Model

Natural fractures intersecting the wellbore through which mud loss and gain occur are modeled as initially closed weak planes with low material strength. Hydraulic fractures initiate and propagate along these weak planes when the ECD in wellbore annulus during drilling exceeds the strength of weak planes (Chuanliang et al., 2014; Feng et al., 2016; Feng and Gray, 2017c; Yan et al., 2014). With pumps off, the fractures will gradually close under negative net pressure.

The cohesive zone model (CZM) is used to simulate the mechanical behavior of the fractures (Zhu et al., 2015). The fracturing process in CZM is represented as the damage evolution between two initially bonded interfaces with zero interfacial thickness. The constitutive response of CZM is characterized by a traction-separation damage law, which consists of three phases: initial loading before damage, damage initiation, and damage evolution. Fig. 2 is a diagram of the traction-separation law used in this study. The initial loading process before the traction reaches cohesive strength T_o of the material follows linear elastic behavior, controlled by stiffness K_0. Damage initiation occurs when traction reaches T_o. After initiation, damage evolution will occur, characterized by a progressively degraded stiffness, K_d. A scalar damage variable is used to represents the damage of the interface in the numerical model. The variable has an initial value of 0 and monotonically evolves from 0 to 1 upon further loading from damage initiation to complete failure of the interface.

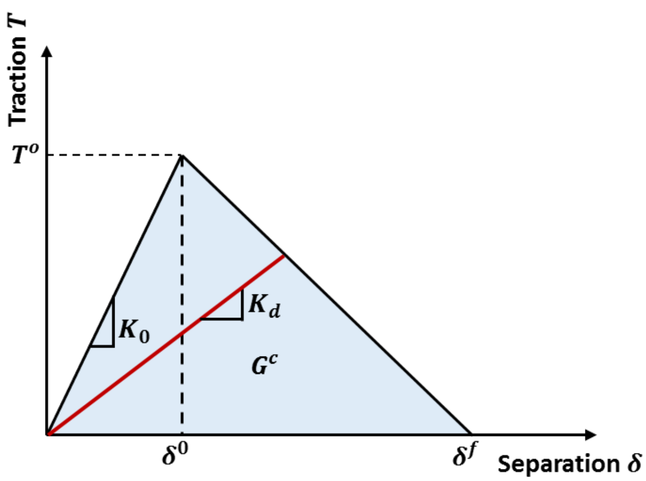

Fig. 2 Traction-separation damage law.

Fluid flow in the fracture is incorporated into the CZM to capture the influence of fracture fluid on the mechanical behavior of the fracture. As the damage initiates and evolves, fluid flow in the cohesive interface is modeled as a transition from Darcy flow to Poiseuille flow, approximating the changes of fluid flow through an initially undamaged porous material to flow in a fracture as the material is damaged. Fluid flow in the fracture includes two components: longitudinal flow along the fracture and normal flow (leak-off) from the fracture surfaces to the surrounding porous medium. Mass conservation of fluid inside the fracture is governed by Reynold's lubrication theory. Longitudinal flow in the fracture is modeled as Poiseuille flow between two narrow parallel plates. Fluid leak-off on the fracture surface is controlled by a leak-off coefficient for the pore fluid material, which defines a pressure-flow relationship between the fluid within the fracture and the pore fluid in the matrix adjacent to the fracture surface.

Formation Deformation and Pore Fluid Flow

Deformation of the porous formation and pore fluid flow in the formation are modeled using the poroelastic model in Abaqus based on Biot's theory (Biot, 1956). The formation rock is assumed to be an isotropic and poroelastic medium, consisting of a solid skeleton and pores saturated with a single-phase fluid. Fluid flow in the pores obeys Darcy's law. The poroelastic theory is a well-established theory and can be found in many standard textbooks, e.g. Jaeger et al. (2007) and Zienkiewicz, et al. (1999).

Model Formulation

Borehole ballooning in a vertical wellbore is considered. The formation is assumed in a 2D, plane-strain condition with unit thickness, as shown in Fig. 3. The wellbore is modeled as a 'U-tube' geometry with the left and right side of the U-tube representing drill pipe and wellbore annulus, respectively. During mud circulation, a fluid pump rate is applied to the top of the drill pipe. The pump rate is then reduced to zero in the pump-off period. Owing to symmetry, only one-half of the formation is modeled. The path of a natural fracture is predefined perpendicular to the direction of the minimum horizontal stress and intersecting with the wellbore as shown in Fig. 3.

A uniform initial pore pressure is applied to the formation. The minimum and maximum horizontal stress is applied in the x- and y- direction, respectively. A symmetric boundary condition is defined on the left edge of the model. The normal displacements of all the other external boundaries are restricted, and the pore pressure at these boundaries is restricted to the initial pore pressure during the entire simulation. Table 1 summaries the input parameters as well as the material properties used in this study.

The end nodes of the wellbore annulus is connected to the nodes on the wellbore wall to ensure fluid conservation between the wellbore and the formation. In addition, another special constraint is imposed to assure the external force acting on the wellbore wall is equal to the fluid pressure at the bottom of the annulus during the simulations. The calculations are done using the Abaqus solver, which is an implicit, general-purpose, finite-element solver.

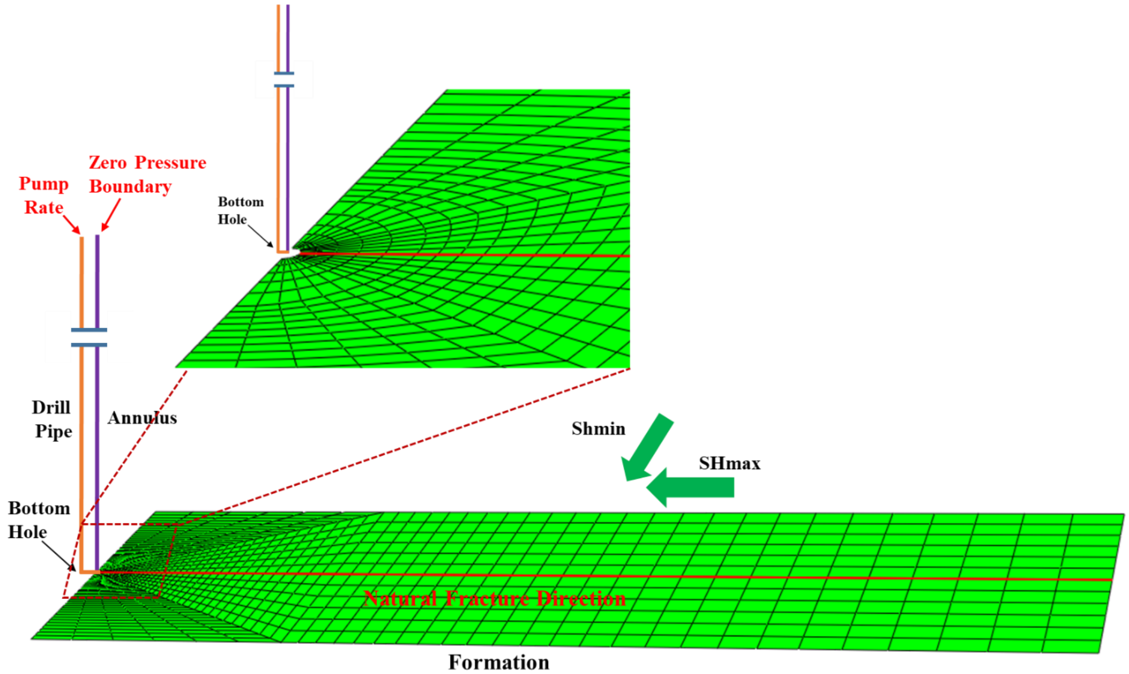

Fig. 3. The borehole ballooning model.

Table 1. Input parameters for the borehole ballooning model.

Parameters	Values	Parameters	Values
Formation size	60 × 20 m	Rock Young's modulus	7 GPa
Formation depth	1000 m	Rock Poisson's ratio	0.2
Wellbore radius	10 cm	Rock permeability	5 mD
Drilling pipe radius	5 cm	Rock porosity	0.25
Annulus clearance	5 cm	Cohesive strength	0.4 MPa
Initial pore pressure	10 MPa	Fracture toughness	28 J/m^2
Minimum horizontal stress	13 MPa	Leak-off coefficient	5×10^{-9} m/s/Pa
Maximum horizontal stress	15 MPa	Interface stiffness	80 GPa
Pore fluid density	1000 Kg/m^3	Pumping rate	0.36 m^3/min
Drilling mud density	1300 Kg/m^3	Mud viscosity	10 cp
Gravity constant	10 m/s^2	Natural fracture length	15 m

Results

Contrary to some existing models that only model fracture itself with a given aperture, the proposed model allows for the hydraulic fracture to grow and close with time-dependent aperture and length controlled by complex interactions between mud circulation, fracture fluid flow, fluid leak-off, and rock deformation. A wealth of information can be provided by the model, including the fluid loss/gain rate, downhole pressure, fracture profile, as well as the pressure and stress distribution in the local area. This section presents some simulation results using input data reported in Table 1. For illustration purpose, a mud circulation period of 50 s and a pump-off period of 100 s are considered.

Fig. 4 shows the downhole pressure during the borehole ballooning event. After the start of mud circulation, the downhole pressure increases rapidly from a hydrostatic pressure of 12 MPa to a dynamic circulation pressure of 15.5 MPa. This circulation pressure is higher than the reopening pressure of the natural fracture. Therefore, the fracture opens as shown in Fig. 5, and consequently, mud flows into the fracture as shown in Fig. 6. Note that in Fig. 6, the positive rate means mud loss from the borehole into the formation during mud circulation, and the negative rate is the rate of mud gain at the wellhead with pumps off.

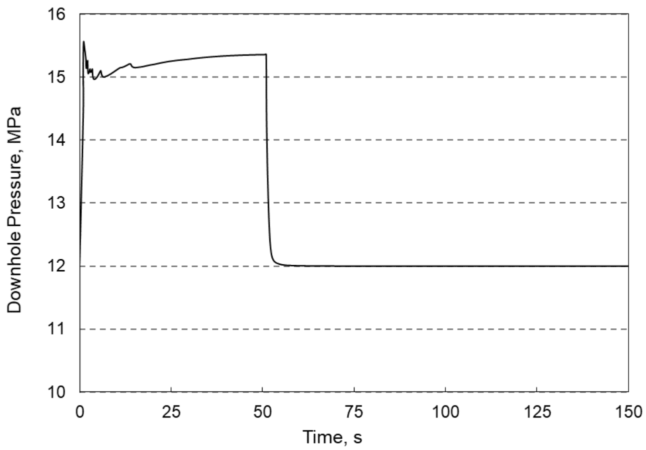

Fig. 4 Downhole pressure vs. time during the wellbore ballooning event.

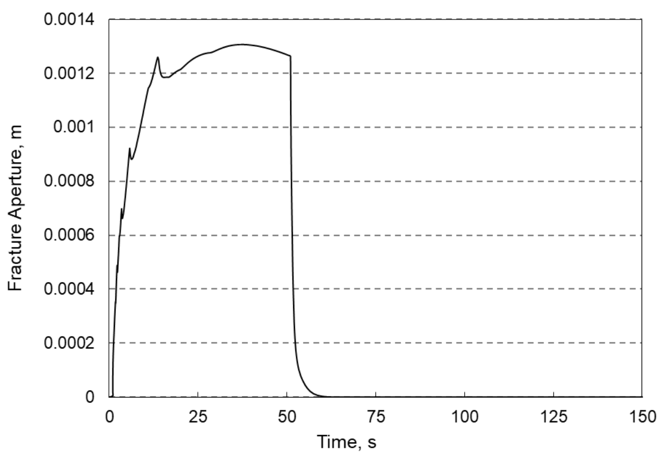

Fig. 5 Fracture mouth aperture vs. time during the wellbore ballooning event.

Fig. 4 indicates that the downhole pressure decreases after the initiation of the natural fracture. At the early time of fracture propagation, downhole pressure fluctuations are observed. This downhole pressure behavior is a part of the solution of the simulation, which is quite different from some existing models that assume a constant downhole pressure (as an input) during mud loss. The fracture extends to the end of the natural fracture at about 20 s. After that, the downhole pressure, fracture width, and mud loss rate reach relatively constant values with continuing mud circulation. At this period, the mud loss rate is dominated by fluid leak off into formation, rather than by fracture growth.

With pumps stopped, the downhole pressure drops almost immediately to the hydrostatic pressure of 12 MPa. As a result, the fracture aperture decreases to zero, but at a rate slower than the decrease of downhole pressure. With fracture closing, fluid flows out of the wellbore with a gradually decreased rate as shown in Fig. 6.

Fig. 7 illustrates the cumulative fluid volume lost into the formation with time during the circulation and pump-off periods, which is the time integral of the flow rate in Fig. 6. The total amount of mud lost into the formation during drilling period is about 0.025 m^3, while the final fluid loss at the end of pump-off period is 0.015 m^3, indicating a fluid gain of 0.01 m^3 after the stop of drilling. The fluid volume that does not return during pump-off period is the part of fluid filtration into the formation. The results demonstrate that the proposed model can simulate the entire process of a borehole ballooning event.

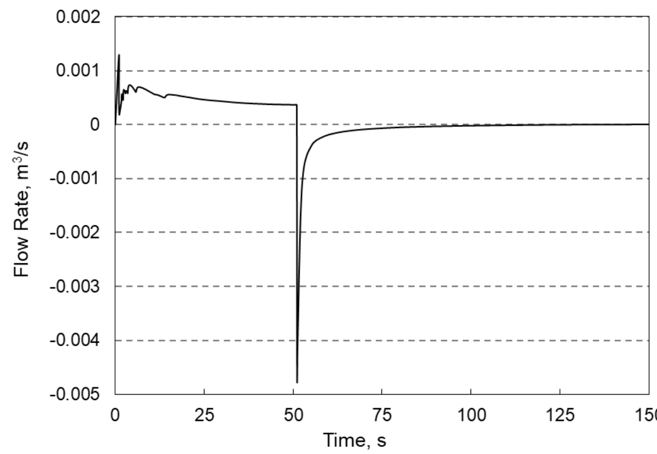

Fig. 6 Fluid loss/gain rate vs. time during the wellbore ballooning event.

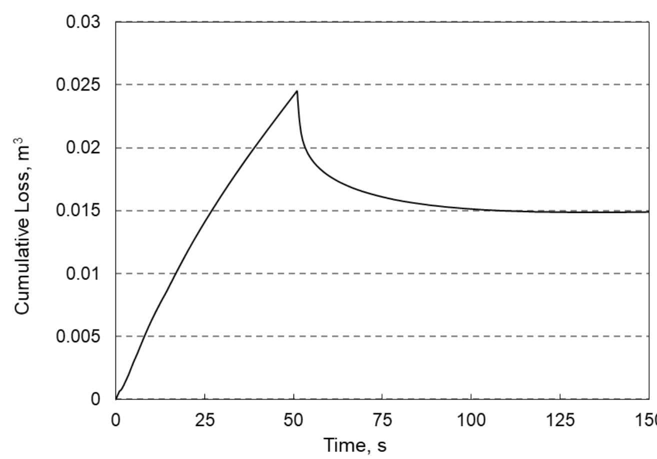

Fig. 6 Cumulative fluid loss vs. time during the wellbore ballooning event.

Conclusions

Modeling borehole ballooning is a challenging endeavor due to strong interactions between wellbore hydraulics, fracture opening/closing, and formation deformation. This paper proposes a numerical model which for the first time takes into account the non-linear coupling between these phenomena in borehole ballooning. The model is able to capture dynamic fracture growth during mud circulation when downhole ECD is higher than fracture reopening pressure of natural fractures, as well as fracture closure during the pump-off period when downhole pressure is lower. Time-dependent wellbore pressure, fluid loss/gain rate, and fracture profile in borehole ballooning can be obtained. The developed model aids in understanding the mechanisms involved in wellbore ballooning in naturally fractured formations. It can be used to investigate the effects of various operational and in-situ parameters on wellbore ballooning, and aids in mud optimization and drilling operations.

Acknowledgments

The authors wish to thank the Wider Windows Industrial Affiliate Program, the University of Texas at Austin, for financial and logistical support of this work. Program support from BHP Billiton, British Petroleum, Chevron, ConocoPhillips, Halliburton, Marathon, National Oilwell Varco, Occidental Oil and Gas, and Shell are gratefully acknowledged.

References

Biot, M.A., 1956. General solutions of the equations of elasticity and consolidation for a porous material. J. Appl. Mech. 78, 91–96.

Bychina, M., Thomas, G.M., Khandelwal, R., Samuel, R., 2017. A Robust Model to Estimate the Mud Loss into Naturally Fractured Formations. Presented at the SPE Annual Technical Conference and Exhibition, Society of Petroleum Engineers. https://doi.org/10.2118/187219-MS

Chuanliang, Y., Jingen, D., Xiangdong, L., Xiaorong, L., Yongcun, F., 2014. Borehole Stability Analysis in Deepwater Shallow Sediments. J. Energy Resour. Technol. 137, 012901-012901-7. https://doi.org/10.1115/1.4027564

Feng, Y., Arlanoglu, C., Podnos, E., Becker, E., Gray, K.E., 2015. Finite-Element Studies of Hoop-Stress Enhancement for Wellbore Strengthening. SPE Drill. Complet. 30, 38–51. https://doi.org/10.2118/168001-PA

Feng, Y., Gray, K.E., 2017a. Modeling Lost Circulation Through Drilling-Induced Fractures. SPE J. https://doi.org/10.2118/187945-PA

Feng, Y., Gray, K.E., 2017b. Parameters controlling pressure and fracture behaviors in field injectivity tests: A numerical investigation using coupled flow and geomechanics model. Comput. Geotech. 87, 49–61. https://doi.org/10.1016/j.compgeo.2017.02.002

Feng, Y., Gray, K.E., 2017c. Review of fundamental studies on lost circulation and wellbore strengthening. J. Pet. Sci. Eng. 152, 511–522. https://doi.org/10.1016/j.petrol.2017.01.052

Feng, Yongcun, Gray, K.E., 2016. A fracture-mechanics-based model for wellbore strengthening applications. J. Nat. Gas Sci. Eng. 29, 392–400. https://doi.org/10.1016/j.jngse.2016.01.028

Feng, Y., Gray, K.E., 2016. A Comparison Study of Extended Leak-Off Tests in Permeable and Impermeable Formations. Presented at the 50th U.S. Rock Mechanics/Geomechanics Symposium, American Rock Mechanics Association.

Feng, Y., Jones, J.F., Gray, K.E., 2016. A Review on Fracture-Initiation and -Propagation Pressures for Lost Circulation and Wellbore Strengthening. SPE Drill. Complet. 31, 134–144. https://doi.org/10.2118/181747-PA

Helstrup, O.A., Chen, Z., Rahman, S.S., 2004. Time-dependent wellbore instability and ballooning in naturally fractured formations. J. Pet. Sci. Eng. 43, 113–128. https://doi.org/10.1016/j.petrol.2004.01.001

Jaeger, J.C., Cook, N.G.W., Zimmerman, R., 2007. Fundamentals of Rock Mechanics. Wiley.

Lavrov, A., Tronvoll, J., 2005. Mechanics of Borehole Ballooning in Naturally-Fractured Formations. Presented at the SPE Middle East Oil and Gas Show and Conference, Society of Petroleum Engineers. https://doi.org/10.2118/93747-MS

Lavrov, A., Tronvoll, J., 2004. Modeling Mud Loss in Fractured Formations. Presented at the Abu Dhabi International Conference and Exhibition, Society of Petroleum Engineers. https://doi.org/10.2118/88700-MS

Lietard, O., Unwin, T., Guillot, D.J., Hodder, M.H., 1999. Fracture Width Logging While Drilling and Drilling Mud/Loss-Circulation-Material Selection Guidelines in Naturally Fractured Reservoirs (includes associated papers 75283, 75284, 81590 and 81591). SPE Drill. Complet. 14, 168–177. https://doi.org/10.2118/57713-PA

Majidi, R., Miska, S., Thompson, L.G., Yu, M., Zhang, J., 2010. Quantitative Analysis of Mud Losses in Naturally Fractured Reservoirs: The Effect of Rheology. SPE Drill. Complet. 25, 509–517. https://doi.org/10.2118/114130-PA

Majidi, R., Miska, S.Z., Yu, M., Thompson, L.G., 2008. Fracture Ballooning in Naturally Fractured Formations: Mechanism and Controlling Factors. Presented at the SPE Annual Technical Conference and Exhibition, Society of Petroleum Engineers. https://doi.org/10.2118/115526-MS

Mehrabi, M., Zeyghami, M., Shahri, M.P., 2012. Modeling of Fracture Ballooning in Naturally Fractured Reservoirs: A Sensitivity Analysis. Presented at the Nigeria Annual International Conference and Exhibition, Society of Petroleum Engineers. https://doi.org/10.2118/163034-MS

Ozdemirtas, M., Babadagli, T., Kuru, E., 2009. Experimental and Numerical Investigations of Borehole Ballooning in Rough Fractures. SPE Drill. Complet. 24, 256–265. https://doi.org/10.2118/110121-PA

Ozdemirtas, M., Babadagli, T., Kuru, E., 2007. Numerical Modelling of Borehole Ballooning/Breathing-Effect of Fracture Roughness. Presented at the Canadian International Petroleum Conference, Petroleum Society of Canada. https://doi.org/10.2118/2007-038

Sanfillippo, F., Brignoli, M., Santarelli, F.J., Bezzola, C., 1997. Characterization of Conductive Fractures While Drilling. Presented at the SPE European Formation Damage Conference, Society of Petroleum Engineers. https://doi.org/10.2118/38177-MS

Shahri, M.P., Zeyghami, M., Majidi, R., 2011. Investigation of Fracture Ballooning and Breathing in Naturally Fractured Reservoirs: Effect of Fracture Deformation Law. Presented at the Nigeria Annual International Conference and Exhibition, Society of Petroleum Engineers. https://doi.org/10.2118/150817-MS

Yan, C., Deng, J., Yu, B., Li, W., Chen, Z., Hu, L., Li, Y., 2014. Borehole Stability in High-Temperature Formations. Rock

Mech. Rock Eng. 47, 2199–2209. https://doi.org/10.1007/s00603-013-0496-2

Zhang, G.M., Liu, H., Zhang, J., Wu, H.A., Wang, X.X., 2010. Three-dimensional finite element simulation and parametric study for horizontal well hydraulic fracture. J. Pet. Sci. Eng. 72, 310–317. https://doi.org/10.1016/j.petrol.2010.03.032

Zhu, H., Zhao, X., Guo, J., Jin, X., An, F., Wang, Y., Lai, X., 2015. Coupled flow-stress-damage simulation of deviated-wellbore fracturing in hard-rock. J. Nat. Gas Sci. Eng. 26, 711–724. https://doi.org/10.1016/j.jngse.2015.07.007

Ziegler, F., Jones, J., 2014. Predrill pore-pressure prediction and pore pressure and fluid loss monitoring during drilling: A case study for a deepwater subsalt Gulf of Mexico well and discussion on fracture gradient, fluid losses, and wellbore breathing. Interpretation 2, SB45-SB55. https://doi.org/10.1190/INT-2013-0099.1

Zienkiewicz, O.C. (Ed.), 1999. Computational geomechanics with special reference to earthquake engineering. Wiley, Chichester ; New York.